Journal of Materials Chemistry C

ROYAL SOCIETY OF CHEMISTRY

REVIEW

View Article Online
View Journal | View Issue

Cite this: J. Mater. Chem. C, 2023, 11, 9082

Regioregular polymerized small-molecule acceptors for high-performance all-polymer solar cells

Chuantao Gu, *[ac] Yu Zhao,[ab] Bing Liu,[c] Yong Tian,[a] Yonghai Li,[bd] Shasha Wang,[a] Shuguang Wen,[bd] Jiping Ma[a] and Xichang Bao *[bd]

Received 13th April 2023,
Accepted 18th June 2023

DOI: 10.1039/d3tc01298k

rsc.li/materials-c

All-polymer solar cells (all-PSCs) have attracted increasing attention because of their distinctive features of superior morphological stability and mechanical durability. In recent years, all-PSCs have made rapid progress, thanks to the strategy of using polymerized small molecular acceptors (PSMAs). The isomerization of monomer of fused ring small molecule acceptors (SMAs) derived from the uncertain position of the bromine atoms on terminal groups leads to regiorandom PSMAs. This isomerization effect can significantly affect the absorption spectra, frontier molecular orbital energy level, crystallinity, mobility, and orientation of PSMAs. Integrating PSMAs with regioregularity endows the materials with better absorption coefficients, superior backbone ordering and optimal blend morphology compared to those of their regiorandom counterparts. Benefitting from these advantages, many regioregular PSMAs have been reported, and the PCE of binary single junction all-PSCs has exceeded 18%. In this review, the advances of regioregular PSMAs in the past three years for high-performance all-PSCs are summarized, and the guidelines for future structure design of PSMAs are discussed.

1. Introduction

Harvesting energy directly from sunlight using photovoltaic technology is increasingly recognized as one of the promising ways to address the growing energy crisis. Polymer solar cells (PSCs) have attracted great attention in the recent twenty years.[1] With the rapid development of wide band-gap polymer donors and fused ring small molecule acceptors (SMAs), the power conversion efficiency (PCE) of PSCs has exceeded 19%.[2,3] Different from SMA-based PSCs, all-polymer solar cells (all-PSCs) with an n-type conjugated polymer as the electron acceptor and a p-type conjugated polymer as the electron donor provide distinctive merits of outstanding morphological stability, remarkable mechanical flexibility, excellent stretchability and mechanical durability.[4–7] These distinctive features make them promising candidates for wearable and portable electronics.

[a] School of Environmental and Municipal Engineering, Qingdao University of Technology, Qingdao 266520, China. E-mail: guchuantao@qut.edu.cn
[b] CAS Key Laboratory of Bio-based Materials, Qingdao Institute of Bioenergy and Bioprocess Technology, Chinese Academy of Sciences, Qingdao 266101, China. E-mail: baoxc@qibebt.ac.cn
[c] State Key Laboratory of Bio-Fibers and Eco-Textiles (Qingdao University), Qingdao 266071, China
[d] Functional Laboratory of Solar Energy, Shandong Energy Institute, Qingdao 266101, China

Chuantao Gu

Chuantao Gu received his PhD from Qingdao Institute of Biomass Energy and Bioprocess Technology, Chinese Academy of Sciences in 2016, and joined Qingdao University as a lecturer in the same year. In 2020, he joined Qingdao University of Technology as an associate professor. His research interests focus on organic photovoltaic materials.

Yu Zhao

Yu Zhao received her BA from Nantong University Xinglin College in 2021. She is pursuing her MS at the School of Environmental and Municipal Engineering, Qingdao University of Technology. Her research interests focus on environmental functional materials.

Since the first reported PSCs using the n-type conjugated polymer CN-PPV as the acceptor,[8] many electron-deficient building blocks have been developed and employed to construct polymer acceptors. Naphthalene diimide (NDI),[9,10] perylene diimide (PDI),[11,12] bithiophene imide (BTI),[13,14] boron–nitrogen coordination bond (B ← N) unit[15,16] and dicyano-benzothiadiazole (DCNBT)[17,18] were among the most commonly used electron-deficient building blocks before 2017. However, polymer acceptors based on these electron-deficient units have some drawbacks such as weak absorption intensity, narrow absorption range, low-lying energy levels and poor electron mobility.[19] Lack of excellent polymer acceptors leads to lower PCEs for all-PSCs than that of SMA-based PSCs.[5,20,21] Further advancements of all-PSCs require new design strategies to develop novel polymer acceptors which should simultaneously possess suitable energy levels, strong light harvesting abilities, and high electron mobility and electron affinity.

In order to develop novel polymer acceptors, Li *et al.* proposed a new strategy to polymerize narrow bandgap SMAs in 2017.[22] They polymerized SMA IDIC-16 with a thiophene linkage unit to obtain a new-type polymer acceptor PZ1 (Fig. 2). The absorption spectrum of the PZ1 film is red-shifted by approximately 50 nm compared with that of IDIC-C16. The onset thermal decomposition (at 5% weight loss) temperature of PZ1 is 368 °C, which is higher than that of IDIC-C16 (338 °C). Melting or glass transition was not observed by differential scanning calorimetry in the temperature range of −20 to 280 °C for PZ1. These results indicate that its thermal stability is better than that of IDIC-16. Crystalline morphology was observed for the optimized PBDB-T:PZ1 film as can be seen from the diffraction patterns with significantly stronger peak intensity along with narrower peak width in their grazing-incidence wide-angle X-ray scattering (GIWAXS) images. The highly crystalline morphology can improve the carrier transport. Benefiting from the extended π conjugation, better light harvesting and better morphological stability, all-PSCs based on PBDB-T:PZ1 yielded a PCE of 9.19%, which is a significant improvement compared to the PCE of 3.96% for the corresponding IDIC-C16-based device.[22] Polymerized SMAs (PSMAs) have received increasing attention as they preserve the merits of SMAs and the good film-forming properties and light-irradiation stability of polymers.[23,24] More importantly, numerous SMA building blocks and different conjugated linkage units can be selected to tune the physicochemical and photovoltaic properties of PSMAs.[19,25–27] Benefitting from these advantages, PSMAs have made rapid development and the related PCEs based on PSMA acceptors derived from Y-series SMAs have reached 18%.[28–30]

Despite the great progress in PSMAs, it should be noted that most PSMAs are synthesized from mixtures of two monomers with IC-Br-γ or IC-Br-δ (Fig. 1) terminal groups,[31,32] which would negatively affect the batch-to-batch reproducibility of PSMAs.[4,33–35] More importantly, the regiorandom polymer backbone significantly disturbs the molecular configuration and electronic structure, which will affect the intermolecular π-stacking, resulting in a significant decrease in its mobility.[25,36] Therefore, a facile way to obtain highly purified brominated terminal groups is urgently required to control the regioregularity of the polymer chain.

In order to solve the regioisomeric issue, Li *et al.* replaced phenyl-fused malononitrile (IC-Br-γ and IC-Br-δ) with thienyl-fused malononitrile (TCN-α and TCN-β, Fig. 1) in 2020.[34] TCN-α and TCN-β can be separated by column chromatography. They designed and synthesized two regioregular PSMAs (PBI-α and PBI-β, Fig. 3) with TCN-α and TCN-β as the terminal group. All-PSCs based on PM6:PBI-α and PM6:PBI-β yielded PCEs of 11.4% and 11.3%, respectively. In the same year, Yang *et al.* separated the isomeric terminal groups IC-Br-γ and IC-Br-δ by chemical recrystallization (Fig. 1),[4] and IC-Br-γ and IC-Br-δ were employed as the terminal group to synthesize two regioregular PSMAs (PY-IT and PY-OT, Fig. 3) and a random ternary copolymer (PY-IOT, Fig. 2) for comparison. The absorption peaks of PY-OT, PY-IOT and PY-IT in chloroform solution are gradually red-shifted, which could be the result of the enhanced lowest unoccupied molecular orbital (LUMO) delocalization. The maximum extinction coefficient of PY-IT in dilute chloroform solution (10^{-5} M) is 1.79×10^4 M^{-1} cm^{-1} at 789 nm, which is slightly higher than those of PY-OT (1.58×10^4 M^{-1} cm^{-1} at 763 nm) and PY-IOT (1.67×10^4 M^{-1} cm^{-1} at 777 nm). The PM6:PY-IT blend yields the highest quenching efficiency of 89.6% (PM6:PY-OT, 40.2%; PM6:PY-IOT, 64.7%), indicating that the hole transfer from PY-IT to the donor polymer PM6 is the most effective

Yonghai Li

Yonghai Li received his PhD from the Institute of Chemistry, Chinese Academy of Sciences (CAS) in 2014. From 2014, he has been working at Qingdao Institute of Biomass Energy and Bioprocess Technology, CAS, first as a postdoctoral fellow (2014–2016), and then as an assistant professor and associate professor. His research interests focus on organic photovoltaic materials.

Xichang Bao

Xichang Bao is a professor at Qingdao Institute of Bioenergy and Bioprocess Technology (QIBEBT), Chinese Academy of Sciences (CAS). He received his PhD from Shanghai Institute of Technical Physics, CAS, in 2010. Since then, he has been working at QIBEBT, CAS. His current research interests include photovoltaics and functional composite materials.

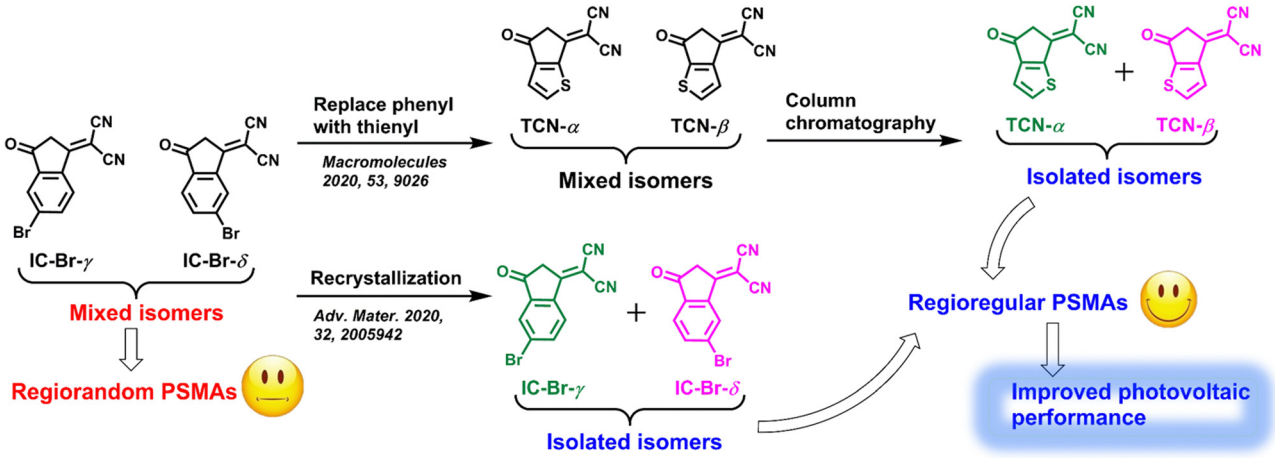

Fig. 1 Separation of terminal group isomers for regioregular PSMAs.

among the three polymer acceptors, which is beneficial to exciton dissociation. The exciton dissociation efficiency (P_{diss})/charge collection efficiency (P_{coll}) values are 90.7%/80.0% for the PY-IT-based device, 87.5%/68.3% for the PY-OT-based device, and 89.2%/72.0% for the PYIOT-based device. The highest P_{diss} and P_{coll} values imply the most effective exciton dissociation and charge collection in the PY-IT-based device. The carrier mobilities of PY-IT are higher and more balanced compared with those of PY-OT and PY-IOT, which could contribute to better J_{SC} and FF in the PY-IT-based device. The morphology of active layers was probed by GIWAXS, grazing-incidence small-angle X-ray scattering (GISAXS) and atomic force microscopy (AFM); the results indicated that the blend of PM6:PY-IT showed a more favorable morphology with a suitable domain size. It can be seen that different polymerization sites have an important effect on the properties of the polymer. The regioregular PY-IT-based all-PSCs achieved a significantly higher PCE (15.05%) than the devices based on regioregular PY-IT (10.04%) and regiorandom PY-IOT (12.12%), which was mainly ascribed to the increased J_{SC} and FF. Hou and co-workers employed the regioregular PY-IT as the polymer acceptor to fabricate all-PSCs, which yielded promising PCEs higher than 18%.[28–30] These results showed that higher charge mobility, more balanced charge transport, and more favorable morphology can be obtained for all-PSCs with regioregular PSMAs as the acceptor.[4,34] Inspired by the exciting results, more regioregular PSMAs[5,35,37–39] have been designed and synthesized to minimize the efficiency gap between the PSCs based on SMAs and PSMAs.

In this review, the recent advances of regioregular PSMAs for high-performance all-PSCs are summarized, and the guidelines for future structure design of PSMAs are discussed.

2. Recent advances of regioregular PSMAs

The prominent factors that restrict the current PCEs of all-PSCs are relatively large E_{loss} (>0.55 eV) and low J_{SC} (normally <25 mA cm^{-2}). Therefore, further efforts are needed to suppress radiative recombination loss to reduce E_{loss} and boost the light absorption in the near-infrared region to enhance J_{SC}.[36]

PSMAs are generally polymerized from an SMA and another aromatic building unit, so they have high structural diversity with large room for molecular modification.[33] Since the first report on high-performance regioregular PSMA, numerous diverse structural variants have appeared[7,40] and the PCEs of binary single junction all-PSCs have been increased to 18%.[28,30,41] Some effective strategies for designing high-performance regioregular PSMAs were developed, including core fused-ring engineering,[5,40,42] terminal group engineering,[6,43] linkage unit modulation[35,44,45] and side chain engineering.[33,39]

2.1 Core fused-ring engineering

The optimization of cores plays a key role in optical absorption, energy levels and molecular packing. The electronic properties of π-conjugated cores can be tailored by modifying the relative electron-deficient strength of the moieties. And core fused-ring engineering is an effective strategy that is commonly used to fine-tune absorption and molecular planarity.[5,40,42] With the uncertain factors in molecular properties and synthetic difficulties, the core fused-ring engineering is considered as one of the most challenging strategies for designing high-performance acceptors, which is endowed with more possibilities to break the bottlenecks.[46]

Enhancing intramolecular charge transfer through enhancing the electron-donating ability of a core fused-ring is an efficient method to extend NIR absorption up to 1000 nm. Jen and co-workers developed a narrow-bandgap regiorandom PSMA named PZT (Fig. 2) and a regioregular PSMA named PZT-γ (Fig. 3) by replacing a strong electron-deficient BT-core fused-ring with a less electron-deficient BTz-core fused-ring.[5] The regiorandom PYT based on a BT-core fused-ring was also synthesized for comparison. The introduction of a less electron-deficient BTz-core fused-ring renders PZT with significantly red-shifted optical absorption and up-shifted energy levels. As a result, all-PSCs based on PZT show simultaneously enhanced V_{OC} and J_{SC}, as well as a reduced nonradiative recombination loss, yielding a decent PCE of 14.5%,

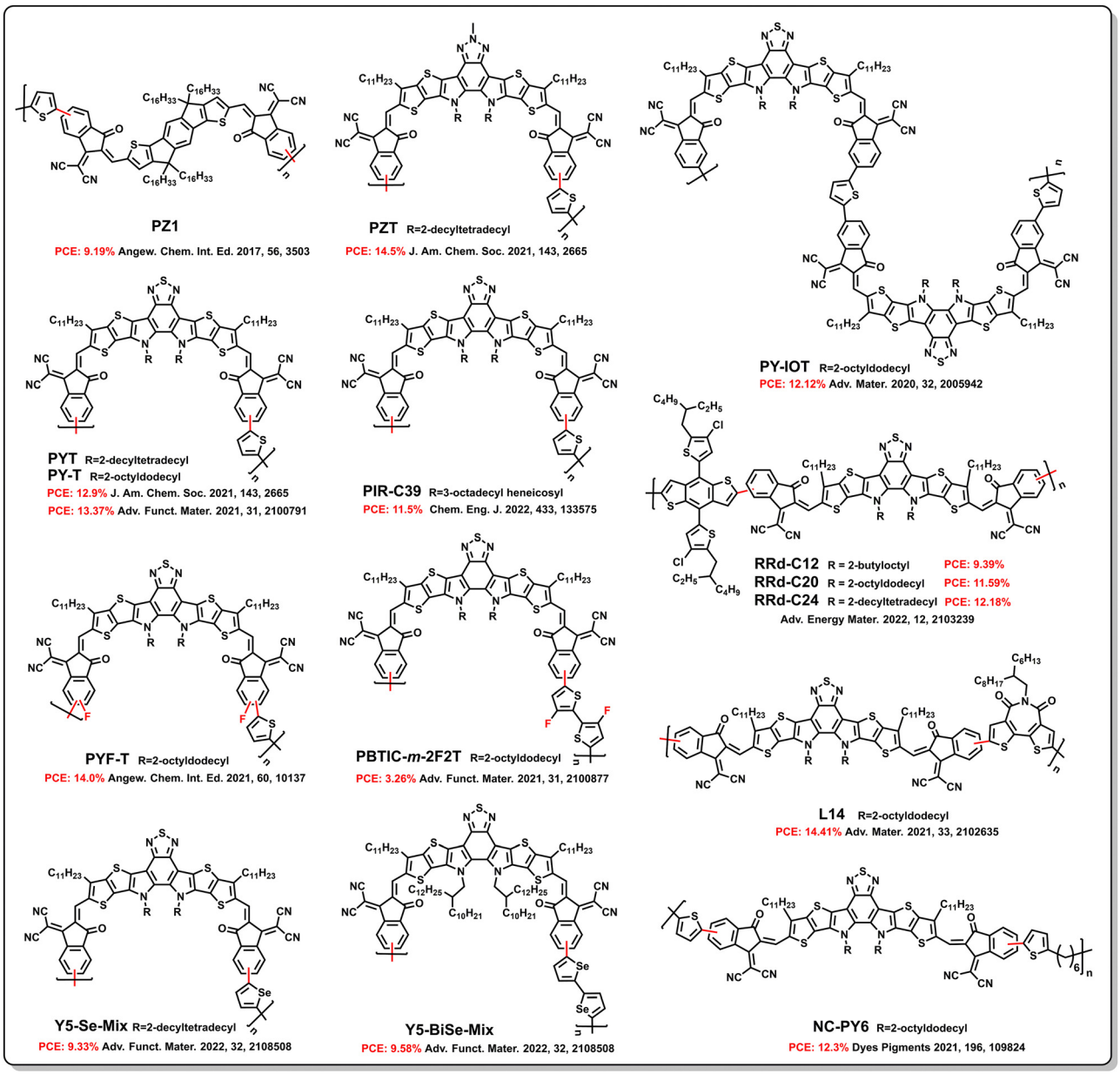

Fig. 2 Chemical structures of the representative regiorandom PSMAs.

which is much higher than that of PYT-based devices (12.9%). More encouragingly, the regioregular PZT-γ renders the PSMA more intense and extended absorption, better backbone ordering and more optimal blend morphology with donor compared to those achieved from regiorandom PZT. The all-PSCs based on PZT-γ show a high PCE of 15.8% with greatly enhanced J_{SC} of 24.7 mA cm^{-2} and a small E_{loss} of 0.51 eV.

Compared with thiophene, selenophene has the characteristics of high polarizability and reduced aromaticity, which could enhance intermolecular interactions and carrier transport and reduce bandgap.[40] In order to manipulate optical absorption and electronic properties, Jen and co-workers designed and synthesized a novel regioregular PSMA named PYT-1S1Se (Fig. 3) by inserting an asymmetrical selenophene-substituted Y6-derivative as the core building block.[40] Regioregular symmetrical PYT-2S (Fig. 3) and PYT-2Se (Fig. 3) were also synthesized for comparison. Benefited from higher EQE values, enhanced electron and hole mobilities, mitigated trap-assisted recombination and reduced E_{loss}, all-PSCs based on PYT-1S1Se show a high PCE of 16.3% with greatly enhanced J_{SC} of 24.1 mA cm^{-2} and a small E_{loss} of 0.502 eV, which is higher than that of the related PYT-2S and PYT-2Se devices (14.8% and 5.5%).

2.2 Terminal group engineering

Core fused-ring engineering has been widely used to tune the intermolecular packing and photovoltaic properties of both SMAs and PSMAs, while terminal group engineering has received relatively less attention due to the synthetic challenge

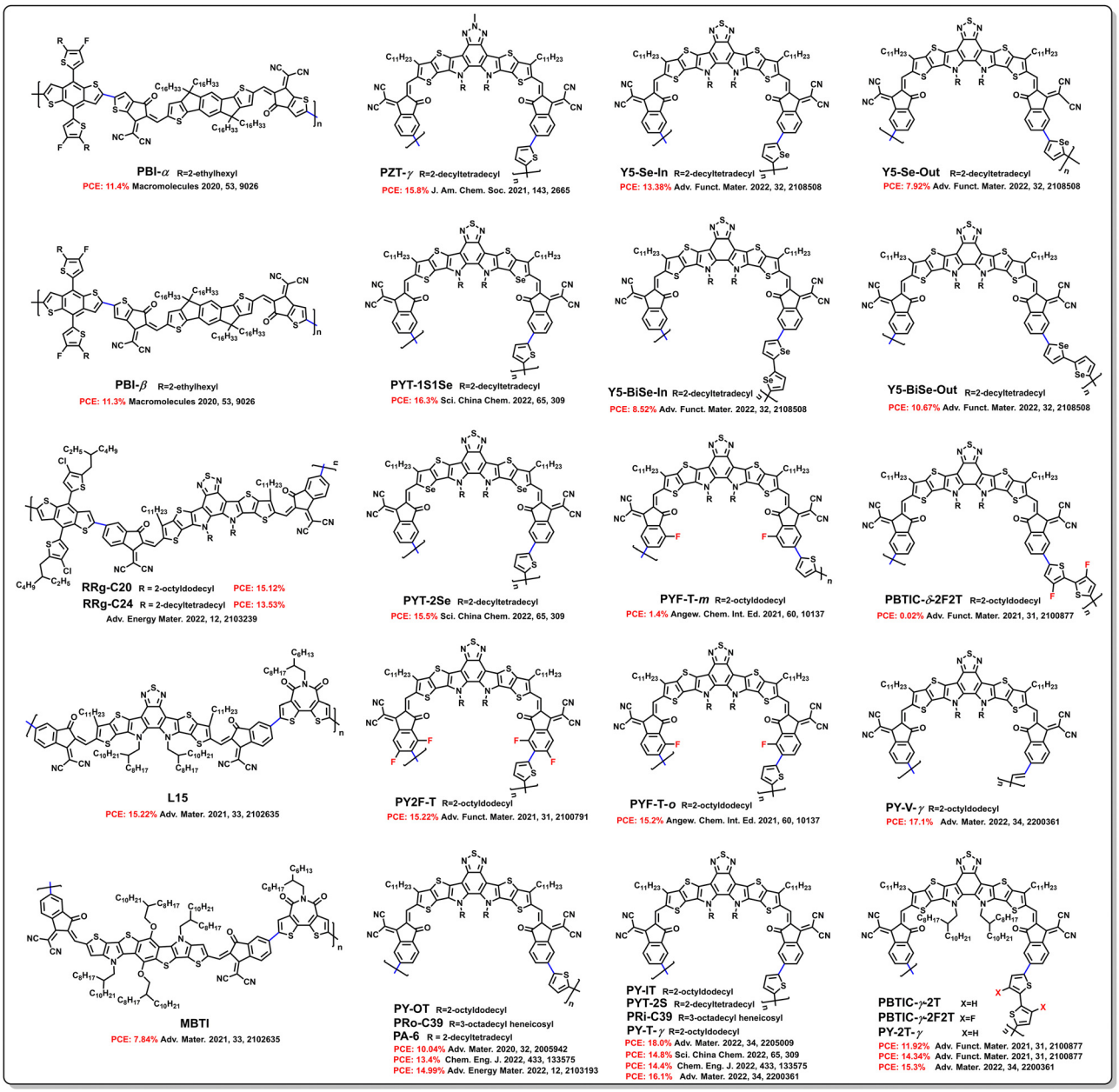

Fig. 3 Chemical structures of representative regioregular PSMAs.

and limited attached positions.[47,48] Halogenation of terminal groups with different numbers of halogen atoms or in different attached positions is commonly used to regulate the electron push–pull capacity, modulate the molecular energy level and blend morphology, which has obvious advantages in improving device performance.[49]

Yan and co-workers designed and synthesized two regioregular PSMAs named PYF-T-*o* and PYF-T-*m* (Fig. 3) with fluoro- and bromosubstituted 1,1-dicyanomethylene-3-indanone (IC-FBr-*o* or IC-FBr-*m*) as the terminal groups.[6] Compared with the regiorandom PYF-T (Fig. 2) and regioregular weak conjugated PYF-T-*m*, the regioregular PYF-T-*o* shows stronger and bathochromic absorption, and achieves better photon harvesting. At the same time, the blend film of PYF-T-*o* and PM6 exhibits more ordered inter-chain packing and suitable phase separation, which can enhance exciton separation, suppress charge recombination, improve charge transfer and reduce E_{loss}. As a result, the all-PSC based on PM6:PYF-T-*o* yields a promising PCE of 15.2%, which is higher than that of the related regiorandom PYF-T (14.0%). They also designed a difluoro-monobromo terminal group IC-2FBr, which is employed to construct a novel regioregular PSMA named PY2F-T.[43] The J_{SC} and FF of all-PSCs based on PM6:PY2F-T are simultaneously enhanced, and the devices yield a PCE of 15.22%, which outperforms that of the devices based on regiorandom PY-T (13.37%).

2.3 Linkage unit modulation

With the great success of Y-series SMAs, they have been widely employed as acceptor units to construct high-performance

PSMAs with different linkage units. The linkage units could affect the molecular configuration, optoelectronic properties, interchain stacking and mobility of PSMAs.[35,41] Nevertheless, most reports are mainly based on thiophene and BDT-based linkage units, while other choices of linkage units have been rarely explored in this family of PSMAs, so far.[19,41]

He *et al.*[35] employed bithiophene and fluorinated bithiophene as linkage units and synthesized three regioregular PSMAs named PBTIC-γ-2F2T, PBTIC-δ-2F2T, and PBTIC-γ-2T (Fig. 3) and one regiorandom PSMA named PBTIC-*m*-2F2T (Fig. 2). Their results show that γ-position PSMA PBTIC-γ-2F2T has proper crystallinity and good miscibility with polymer donors, and the all-PSC based on PBTIC-γ-2F2T yields a PCE of 14.34%. Kim and co-workers investigated the crystalline and optoelectrical properties of six PSMAs with different regioregularities (in, mix, and out) and linkage units (selenophene and biselenophene).[44] All-PSCs based on these PSMAs yield PCEs ranging from 7.92 to 13.38%. Yan *et al.*[41] designed and synthesized a series of regioregular PSMAs named PY-V-γ, PY-T-γ and PY-2T-γ (Fig. 3) with vinylene, thiophene and bithiophene as the linkage units, respectively. Benefited from a more coplanar and rigid molecular conformation, PY-V-γ exhibits a better conjugation and tighter molecular stacking, which render the PY-V-γ higher mobility and reduced energetic disorder. The binary all-PSC based on PY-V-γ yields a promising PCE of 17.1%.

Guo and co-workers employed electron-withdrawing bithiophene diimide (BTI) as the linkage unit for the first time,[50] and synthesized a regioregular PSMA L15 (Fig. 3)[45] and regiorandom PSMA L14 (Fig. 2) for comparison. It can be found that the introduction of BTI could improve the electron transport properties of PSMAs. The regioregular backbone renders L15 superior backbone ordering and optimal blend morphology compared to those achieved using regiorandom L14. The all-PSC based on PM6:L15 yields a PCE of 15.2%, which is higher than that of the PM6:L14-based devices (14.4%). This work demonstrates that the systematic engineering of linkage units and regioregularity of PSMAs can effectively enhance electron mobility and realize high-performance all-PSCs.

Chen and co-workers designed and synthesized a new regiorandom PSMA named NC-PY6 (Fig. 2) with a non-conjugated alkyl chain as the linkage unit.[51] NC-PY6 exhibits a narrow bandgap of 1.44 eV and low-lying LUMO of −3.92 eV, which match with those of the polymer donor D18. The all-PSCs based on D18:NC-PY6 gave an encouraging PCE of 12.3% with an E_{loss} of 0.57 eV. Combined engineering of a non-conjugated linkage unit and regioregularity could be an effective design strategy of PSMAs.

2.4 Side chain engineering

Side chain engineering is another commonly used and effective strategy to improve the photovoltaic performance of materials. Side chains attached to conjugated systems can not only regulate the solubility, but also alter their electronic properties since alkyl chains are weakly electron donating *via* the inductive effect.[46] Simultaneous engineering of the backbone regioregularity and side-chain structures of PSMAs can efficiently yield favorable crystallinity, provide a suitable mixing phase, enhance electron mobility, optimize blend morphology and achieve high-performance all-PSCs.[33]

In order to regulate the crystalline and aggregation properties of PSMAs, Kim and co-workers developed a series of PSMAs (regiorandom RRd-C12, RRd-C20, RRd-C24 (Fig. 2), and regioregular RRg-C20, RRg-C24 (Fig. 3)) with simultaneously-engineered side chain lengths and backbone regioregularities.[33] Due to the high crystallinity and optimal blend morphology, all-PSCs based on regioregular RRg-C20 yielded the highest PCE of 15.12%. Huang *et al.* synthesized two regioregular PSMAs (PRi-C39 and PRo-C39, Fig. 3) and a regiorandom PSMA (PIR-C39, Fig. 2) that can be processed with a non-halogenated solvent by optimizing side chains.[39] The long-branched 3-octadecyl heneicosyl is selected to enhance the solute–solvent interaction and enable the resulting polymer to be dissolved and processable in non-halogenated 2-methyltetrahydrofuran. The results show that higher charge mobility and reduced recombination loss benefited from superior molecular crystallinity and packing, and all-PSCs based on regioregular PRi-C39 and PRo-C39 yield high PCEs of 14.4% and 13.4%, which is higher than that of the regiorandom PIR-C39 (11.5%).

2.5 Molecular weights (MWs)

Molecular weight also has a significant impact on the performance of polymers. Min *et al.*[52] synthesized a series of regiorandom PSMAs named PYT (Fig. 2) with different MWs to investigate the effect of molecular weight on their photovoltaic performance. When fabricated into all-PSCs with PM6, they observed a clear molecular weight dependence on device performance. The optimized devices based on PYT_L (low MWs, 7.2 kg mol^{-1}), PYT_M (medium MWs, 12.3 kg mol^{-1}), and PYT_H (high MWs, 20.6 kg mol^{-1}) exhibit PCEs of 12.55%, 13.44%, and 8.61%, respectively. Yang *et al.*[7] also synthesized a series of regioregular PA-6 (Fig. 3) with different MWs. The optimized devices based on PA-6_L (low MWs, 12.0 kg mol^{-1}), PA-6_M (medium MWs, 30.4 kg mol^{-1}), and PA-6_H (high MWs, 71.3 kg mol^{-1}) give PCEs of 14.81%, 14.99%, and 12.78%, respectively. From their results we can see that all-PSCs based on PSMAs with low and medium MWs displayed a negligible MW impact on photovoltaic performance. PSMAs with high MWs show poor device efficiency, mainly resulting from the poor solubility and poor morphology with large domains.[7,52] The effects of molecular weight improvement on photovoltaic performance, solubility and morphology should be comprehensively considered when designing PSMAs. The regioregular PA-6 has the same backbone as regiorandom PYT, and the PCE of PA-6 is significantly higher than that of PYT, demonstrating that regioregularity is crucial for improving PCE.

2.6 Applications of regioregular polymers in ternary all-PSCs and single-material PSCs

Ternary strategy has been demonstrated to be an effective way to improve the performance of PSCs *via* introducing a third component into the binary matrix, which can improve photon utilization, broaden spectrum, alter D/A intermolecular interaction, suppress carrier recombination and reduce energy disorder.[29,53] The application of a regioregular polymer in

building ternary all-PSCs[37,38,45,54,55] also achieved promising results.

Min *et al.*[55] fabricated ternary all-PSCs based on PM6:PYT:-PY2F-T (PY2F-T is a regioregular PSMA). Benefited from the complementary absorption and finely tuned microstructures of the ternary blend, the ternary all-PSCs yield a high PCE of 17.2%, with EQE over 80% in the visible and near-infrared spectral regions. Hou *et al.* fabricated ternary all-PSCs based on PBQx-TF:PBDB-TF:PY-IT (PY-IT is a regioregular PSMA). Benefited from shorter π–π stacking distance, more orderly stacking of donors, more efficient exciton generation rate, less energetic disorder and obviously suppressed non-radiative charge recombination, the ternary all-PSCs yield a high PCE of 18.2%, which is the highest value for the reported all-PSCs so far.[29]

The optimal D/A bulk heterojunction (BHJ) blend morphology of binary or ternary all-PSCs is crucial for achieving preferable contact and molecular orientation to achieve charge dissociation and transport. In order to overcome this limitation in BHJ systems, single-material PSCs have been proposed, which can minimize procedures for preparation of devices.[56] Yuan and co-workers designed and synthesized a regioregular block copolymer named PBDB-T-*b*-PTY6-γ,[57] which exhibits a decreased bandgap and enhanced solid film ordering. Single-material PSCs based on regioregular PBDB-T-*b*-PTY6-γ yield enhanced J_{SC} and a champion PCE of 10.51%, which is among the highest reported for single-material PSCs.

The chemical structures of these typical regiorandom PSMAs are shown in Fig. 2 while the chemical structures of regioregular PSMAs are shown in Fig. 3. The relevant device performance values of all-PSCs based on these PSMAs are summarized in Fig. 4 and Table 1. In most cases, if the linkage unit is thiophene,[4,5] bithiophene[35] and selenophene,[44] the performance of the regioregular PSMAs synthesized using IC-Br-γ is better than that of regiorandom PSMAs and regioregular PSMAs synthesized using IC-Br-δ. If the linkage unit is biselenophene,[44] the opposite is true, which originates from the difference in planarity and intermolecular assembly. With fine-tuned structures of regioregular PSMAs, all-PSCs achieve an increased V_{OC} due to well matched energy levels and decreased energy loss, higher J_{SC} and improved fill factor enabled by broadening absorption spectra and enhancing carrier mobility, leading to the state-of-the-art all-PSCs performing quite close to the most efficient SMA-based devices. These exciting results will inspire researchers to devote more efforts to further develop more efficient regioregular PSMAs.

3. Conclusions and prospects

In summary, regioregular PSMAs contribute to boosting absorption in the near-infrared region, yielding superior backbone ordering, stronger inter chain packing and more suitable phase separation. Therefore, precise controlling of the regioregularity of PSMAs is an important and promising strategy to enhance the charge carrier mobility and decrease the π–π stacking distance as well as energy loss, which helps to achieve high-performance all-PSCs. In addition, there are also some notable advantages, such as batch-to-batch reproducibility and reproducible device performance, expanding the possible applications of all-PSCs.

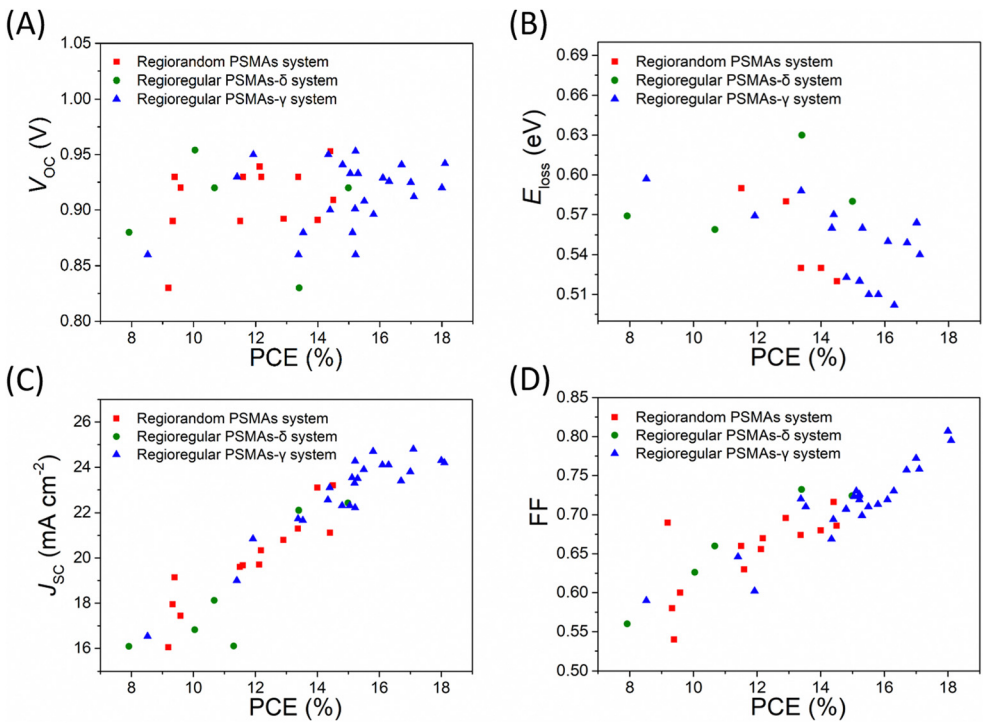

Fig. 4 Comparison of the reported V_{OC} and PCE values (A), E_{loss} and PCE values (B), J_{SC} and PCE values (C), and FF and PCE values (B) for regiorandom PSMAs (red), regioregular PSMAs-δ (green) and regioregular PSMAs-γ (blue) based binary all-PSCs.

Table 1 Summarized parameters of all-PSCs based on regiorandom and regioregular PSMAs

Regioregularity of acceptor	Acceptor	Donor	Ratio (D/A)	V_{OC} [V]	E_{loss} [eV]	J_{SC} [mA cm^{-2}]	FF	PCE [%]	Ref.
No	PZ1	PBDB-T	1.5 : 1	0.830	—	16.05	0.690	9.19	22
Yes	PBI-α	PM6	1.5 : 1	0.930	—	19.0	0.646	11.4	34
Yes	PBI-β	PM6	1.5 : 1	1.030	—	16.1	0.684	11.3	34
Yes	PY-IT	PM6	1 : 1	0.933	—	22.30	0.723	15.05	4
Yes	PY-OT	PM6	1 : 1	0.954	—	16.82	0.626	10.04	4
No	PY-IOT	PM6	1 : 1	0.939	—	19.71	0.656	12.12	4
Yes	PY-IT	PQM-Cl	1 : 1.2	0.920	—	24.3	0.807	18.0	30
Yes	PY-IT	PQB-2	1 : 1	0.942	—	24.2	0.795	18.1	28
Yes	PY-IT	PBDB-TF	1 : 1.2	0.941	0.549	23.4	0.757	16.7	29
Yes	PY-IT	PBQx-TF	1 : 1.2	0.925	0.564	23.8	0.772	17.0	29
No	PYT	PBDB-T	1 : 1	0.892	0.58	20.8	0.696	12.9	5
No	PZT	PBDB-T	1.2 : 1	0.909	0.52	23.2	0.686	14.5	5
Yes	PZT-γ	PBDB-T	1 : 1	0.896	0.51	24.7	0.713	15.8	5
Yes	PYT-2S	PM6	1 : 1	0.941	0.523	22.3	0.707	14.8	40
Yes	PYT-1S1Se	PM6	1 : 1	0.926	0.502	24.1	0.730	16.3	40
Yes	PYT-2Se	PM6	1 : 1	0.908	0.510	23.9	0.714	15.5	40
No	PYF-T	PM6	1 : 1.2	0.891	0.53	23.1	0.680	14.0	6
Yes	PYF-T-*o*	PM6	1 : 1.2	0.901	0.52	23.3	0.724	15.2	6
No	PY-T	PM6	1 : 1.2	0.93	0.53	21.30	0.674	13.37	43
Yes	PY2F-T	PM6	1 : 1.2	0.86	0.52	24.27	0.726	15.22	43
Yes	PBTIC-γ-2F2T	PM6	1 : 1.2	0.95	0.560	22.56	0.669	14.34	35
No	PBTIC-*m*-2F2T	PM6	1 : 1.2	0.99	0.528	9.72	0.338	3.26	35
Yes	PBTIC-γ-2T	PM6	1 : 1.2	0.95	0.569	20.85	0.602	11.92	35
Yes	Y5-Se-Out	PBDB-T	1 : 1	0.88	0.569	16.09	0.56	7.92	44
No	Y5-Se-Mix	PBDB-T	1 : 1	0.89	—	17.95	0.58	9.33	44
Yes	Y5-Se-In	PBDB-T	1 : 1	0.86	0.588	21.74	0.72	13.38	44
Yes	Y5-BiSe-Out	PBDB-T	1 : 1	0.92	0.559	18.12	0.66	10.67	44
No	Y5-BiSe-Mix	PBDB-T	1 : 1	0.92	—	17.44	0.60	9.58	44
Yes	Y5-BiSe-In	PBDB-T	1 : 1	0.86	0.597	16.54	0.59	8.52	44
Yes	PY-V-γ	PM6	1 : 1.2	0.912	0.54	24.8	0.758	17.1	41
Yes	PY-T-γ	PM6	1 : 1.2	0.929	0.55	24.1	0.719	16.1	41
Yes	PY-2T-γ	PM6	1 : 1.2	0.933	0.56	23.5	0.699	15.3	41
No	L14	PM6	1 : 1	0.953	—	21.12	0.716	14.41	45
Yes	L15	PM6	1 : 1.2	0.953	—	22.21	0.719	15.22	45
No	NC-PY6	D18	1 : 1	0.87	—	20.66	0.684	12.30	51
No	RRd-C12	PBDB-T	1 : 1.2	0.93	—	19.14	0.54	9.39	33
No	RRd-C20	PBDB-T	1 : 1.2	0.93	—	19.67	0.63	11.59	33
No	RRd-C24	PBDB-T	1 : 1.2	0.93	—	20.34	0.67	12.18	33
Yes	RRg-C20	PBDB-T	1 : 1.2	0.88	—	23.54	0.73	15.12	33
Yes	RRg-C24	PBDB-T	1 : 1.2	0.88	—	21.67	0.71	13.53	33
Yes	PA-6	JD40	1 : 1	0.92	0.58	22.42	0.724	14.99	7
No	PIR-C39	PTzBI-Si	1 : 1	0.89	0.59	19.6	0.660	11.5	39
Yes	PRi-C39	PTzBI-Si	1 : 1	0.90	0.57	23.1	0.694	14.4	39
Yes	Pro-C39	PTzBI-Si	1 : 1	0.83	0.63	22.1	0.732	13.4	39

The guidelines for future structure design of PSMAs are discussed in the following text.

3.1 Core engineering

Optimization of the core plays a vital role in optical absorption, energy levels, and molecular packing. Decreasing the electron-deficient ability of core is a prospectively efficient way to modulate molecular energy level, optimize molecular stacking and enhance intramolecular charge transfer (ICT).[5] The weak electron-deficient BTz and quinoxaline are candidates to replace the strong electron-deficient BT. At present, most of the cores used are fused ring, which often involved multistep chemical reactions and high costs.[21] These disadvantages make them unfavorable for industrial application. The non-fused ring core has the advantages of simple synthesis, high yields, and low costs. Polymerizing non-fused small molecular acceptors is an effective strategy to develop cost-effective and regioregular PSMAs for future high-performance all-PSCs.

3.2 Terminal group engineering

Terminal group engineering has obvious advantages in adjusting long-range order. Employment of halogenated terminal groups is an effective way to increase intramolecular charge transfer, improve charge mobility and suppress charge recombination.[6,43] The species, position and quantity of halogen have a significant influence on the photovoltaic performance of PSMAs, which need to be further studied. Extending the conjugation and introducing heteroatom into the halogened terminal groups are also potential approaches for further advancing regioregular PSMAs.

3.3 Linkage unit modulation

The commonly used linking units are mostly electron-donating units, such as thiophene, selenophene and BDT derivatives.[35] In addition, the electron-withdrawing units[45] and non-conjugated linkage units[51] can also be used as linkage units. The introduction of electron-withdrawing units as the linkage to form A–A type PSMAs can provide additional electron channels and help

improve the high electron mobility. However, how the linking units affect the intramolecular interaction, intermolecular interaction and molecular configuration of PSMAs is still unclear, and further research is urgently needed.

3.4 Side chain engineering

Precisely optimizing the side chain is a good approach for advancing the performance of photovoltaic materials.[39] There are many studies on the side chain engineering of SMAs, but few studies on that of regioregular PSMAs, such as how the bulk and length of the side chain affect the physical and electrical properties of PSMAs. In addition, some strategies used in side chain engineering of SMAs can also be used for reference in the design of regioregular PSMAs, such as terminal aryl alkyl side chains[58–61] and asymmetric side chains.[62–64]

3.5 Configuration of IC-Br

In most cases, if the linkage unit is thiophene,[4,5] bithiophene[35] and selenophene,[44] the photovoltaic performance increases in the order of regioregular PSMAs synthesized using IC-Br-δ (regioregular PSMAs-δ) < regiorandom PSMAs < regioregular PSMAs synthesized using IC-Br-γ (regioregular PSMAs-γ). If the linkage unit is biselenophene,[44] the photovoltaic performance increase in order of regioregular PSMAs synthesized using IC-Br-γ (regioregular PSMAs-γ) < regiorandom PSMAs < regioregular PSMAs synthesized using IC-Br-δ (regioregular PSMAs-δ). Further research on the effect of configuration of IC-Br on the photovoltaic performance of PSMAs is urgently needed.

3.6 Morphological control

The morphology of the active layer is highly susceptible to the influence of intermolecular interactions and formation processes.[58,61] The weak interactions between conjugated molecules mainly include van der Waals interactions, π–π interactions, hydrogen bonds, and so on. Regioregular PSMAs possess better conjugation along the polymer backbone and more ordered interchain-packing, which is more conducive to exerting the role of intermolecular interactions. Compared with donor polymers:-regiorandom PSMA blends, the donor polymers:regioregular PSMA blends show a smaller Flory–Huggins interaction parameter (χ), which indicates stronger miscibility and improved degree of mixing.[52,55] Thanks to the denser intermolecular stacking and stronger conjugation that stabilize the chemical structure, the morphological stability of the regioregular PSMA-based devices is better than that of regiorandom PSMA-based devices.[6]

The relationship between intermolecular interactions and photovoltaic performance is crucial to the development of organic photovoltaics. And the multidimensional intermolecular interaction mechanism is an important aspect in organic solar cells. The intermolecular interactions at the D/A interface, in the acceptor phase, and between host and guest molecules in the ternary system are not isolated, they synergistically affect the morphology and photoelectric conversion process. How these multidimensional interactions synergistically affect exciton generation, dissociation and charge transfer in the blend, and how to rationally regulate these interactions through molecular design are worthy of an in-depth study in the future.

3.7 Device fabrication

The development of PSCs has now reached the stage where further consideration of cost, stability and processing conditions is required for large-scale commercialization.[65] At present, most of the reported high-efficiency devices are small-area (less than 1 cm^2) devices with an active layer thickness of about 100 nm prepared by spin coating.[21] Optimal blend morphology can be obtained through this fabrication method, but the waste of materials is serious and not suitable for industrial production. Therefore, knife coating, slot-die coating, screen printing, inkjet printing, brush coating and other preparation methods suitable for the fabrication of large-area devices should be adopted in industrial production.[66] The classical BHJ active layer prepared by these methods can achieve large area, but the issues of film thickness uniformity and numerous defects in the active layers can seriously weaken the performance of the related devices.[53] Although the ternary strategy[67,68] shows great potential in relieving the disadvantage of sensitive performance to active layer thickness for PSCs,[53,69] it is difficult to effectively solve the multifaceted problems in the current development of organic photovoltaics. Hence, design and synthesis of high-efficiency acceptors with improved thickness tolerance and suitable for large-area thick-film devices are very important for the large-scale commercialization of PSCs. For example, the acceptors with terminal aryl alkyl side chains designed and synthesized by our research group show outstanding thickness-insensitive behaviors, which are very suitable for fabricating high-efficiency thick-film PSCs.[58,61] In addition, suitable new device structures should be developed to reduce the harsh requirements for film forming processes.

It is only about three years since the first case of regioregular PSMA was reported. Thanks to the rapid development of regioregular PSMAs, the PCE of binary single junction all-PSCs based on regioregular PSMA has exceeded 18%,[28,30] which is a very promising result. We believe that with careful consideration of the above design strategies, the resulting novel regioregular PSMAs could achieve a higher PCE.

Conflicts of interest

There are no conflicts to declare.

Acknowledgements

The authors gratefully acknowledge the National Key R&D Program of China (2021YFE0190400), the National Natural Science Foundation of China (21807062, 22005324, 52002196, 52073122, and 22006085), Department of Science and Technology of Shandong Province (ZR2020MB085), Shandong Provincial Natural Science Foundation (ZR2020QB135), Shandong Energy Institute (SEII202111, SEIS202108), State Key Laboratory of Bio-Fibers and Eco-Textiles (Qingdao University) (no. KFKT202223), and the Shandong Province Higher Educational

Program for Introduction and Cultivation of Young Innovative Talents (2021) for financial support.

References

1 C. Gu, D. Liu, J. Wang, Q. Niu, C. Gu, B. Shahid, B. Yu, H. Cong and R. Yang, *J. Mater. Chem. A*, 2018, **6**, 2371–2378.
2 R. Sun, Y. Wu, X. Yang, Y. Gao, Z. Chen, K. Li, J. Qiao, T. Wang, J. Guo, C. Liu, X. Hao, H. Zhu and J. Min, *Adv. Mater.*, 2022, **34**, 2110147.
3 L. Zhu, M. Zhang, J. Xu, C. Li, J. Yan, G. Zhou, W. Zhong, T. Hao, J. Song, X. Xue, Z. Zhou, R. Zeng, H. Zhu, C. C. Chen, R. C. I. MacKenzie, Y. Zou, J. Nelson, Y. Zhang, Y. Sun and F. Liu, *Nat. Mater.*, 2022, **21**, 656–663.
4 Z. Luo, T. Liu, R. Ma, Y. Xiao, L. Zhan, G. Zhang, H. Sun, F. Ni, G. Chai, J. Wang, C. Zhong, Y. Zou, X. Guo, X. Lu, H. Chen, H. Yan and C. Yang, *Adv. Mater.*, 2020, **32**, e2005942.
5 H. Fu, Y. Li, J. Yu, Z. Wu, Q. Fan, F. Lin, H. Y. Woo, F. Gao, Z. Zhu and A. K. Jen, *J. Am. Chem. Soc.*, 2021, **143**, 2665–2670.
6 H. Yu, M. Pan, R. Sun, I. Agunawela, J. Zhang, Y. Li, Z. Qi, H. Han, X. Zou, W. Zhou, S. Chen, J. Y. L. Lai, S. Luo, Z. Luo, D. Zhao, X. Lu, H. Ade, F. Huang, J. Min and H. Yan, *Angew. Chem., Int. Ed.*, 2021, **60**, 10137–10146.
7 J. Jia, Q. Huang, T. Jia, K. Zhang, J. Zhang, J. Miao, F. Huang and C. Yang, *Adv. Energy Mater.*, 2022, **12**, 2103193.
8 G. Yu and A. J. Heeger, *J. Appl. Phys.*, 1995, **78**, 4510–4515.
9 H. Yan, Z. Chen, Y. Zheng, C. Newman, J. R. Quinn, F. Dotz, M. Kastler and A. Facchetti, *Nature*, 2009, **457**, 679–686.
10 L. Zhu, W. Zhong, C. Qiu, B. Lyu, Z. Zhou, M. Zhang, J. Song, J. Xu, J. Wang, J. Ali, W. Feng, Z. Shi, X. Gu, L. Ying, Y. Zhang and F. Liu, *Adv. Mater.*, 2019, **31**, e1902899.
11 Y. Guo, Y. Li, O. Awartani, J. Zhao, H. Han, H. Ade, D. Zhao and H. Yan, *Adv. Mater.*, 2016, **28**, 8483–8489.
12 Y. Guo, Y. Li, O. Awartani, H. Han, J. Zhao, H. Ade, H. Yan and D. Zhao, *Adv. Mater.*, 2017, **29**, 1700309.
13 Y. Wang, Z. Yan, M. A. Uddin, X. Zhou, K. Yang, Y. Tang, B. Liu, Y. Shi, H. Sun, A. Deng, J. Dai, H. Y. Woo and X. Guo, *Sol. RRL*, 2019, **3**, 1900107.
14 Y. Shi, H. Guo, J. Huang, X. Zhang, Z. Wu, K. Yang, Y. Zhang, K. Feng, H. Y. Woo, R. P. Ortiz, M. Zhou and X. Guo, *Angew. Chem., Int. Ed.*, 2020, **59**, 14449–14457.
15 R. Zhao, B. Lin, J. Feng, C. Dou, Z. Ding, W. Ma, J. Liu and L. Wang, *Macromolecules*, 2019, **52**, 7081–7088.
16 R. Zhao, N. Wang, Y. Yu and J. Liu, *Chem. Mater.*, 2020, **32**, 1308–1314.
17 S. Shi, P. Chen, Y. Chen, K. Feng, B. Liu, J. Chen, Q. Liao, B. Tu, J. Luo, M. Su, H. Guo, M. G. Kim, A. Facchetti and X. Guo, *Adv. Mater.*, 2019, **31**, e1905161.
18 K. Feng, J. Huang, X. Zhang, Z. Wu, S. Shi, L. Thomsen, Y. Tian, H. Y. Woo, C. R. McNeill and X. Guo, *Adv. Mater.*, 2020, **32**, e2001476.
19 C. Gu, X. Su, Y. Li, B. Liu, Y. Tian, W. Tan, J. Ma and X. Bao, *Mol. Syst. Des. Eng.*, 2022, **7**, 1364–1384.
20 J. Du, K. Hu, L. Meng, I. Angunawela, J. Zhang, S. Qin, A. Liebman-Pelaez, C. Zhu, Z. Zhang, H. Ade and Y. Li, *Angew. Chem., Int. Ed.*, 2020, **59**, 15181–15185.
21 C. Gu, X. Wang, H. Wang, Y. Tian, J. Ma and R. Yang, *Mol. Syst. Des. Eng.*, 2022, **7**, 832–855.
22 Z. G. Zhang, Y. Yang, J. Yao, L. Xue, S. Chen, X. Li, W. Morrison, C. Yang and Y. Li, *Angew. Chem., Int. Ed.*, 2017, **56**, 13503–13507.
23 Y. Meng, J. Wu, X. Guo, W. Su, L. Zhu, J. Fang, Z.-G. Zhang, F. Liu, M. Zhang, T. P. Russell and Y. Li, *Sci. China: Chem.*, 2019, **62**, 845–850.
24 L. Zeng, R. Ma, Z. Zhou, T. Liu, Y. Xiao, X. Lu, D. Xue, W. Zhu, H. Yan and Y. Liu, *Chem. Eng. J.*, 2022, **429**, 132551.
25 Z.-G. Zhang and Y. Li, *Angew. Chem., Int. Ed.*, 2021, **60**, 4422–4433.
26 L. Zhang, T. Jia, L. Pan, B. Wu, Z. Wang, K. Gao, F. Liu, C. Duan, F. Huang and Y. Cao, *Sci. China: Chem.*, 2021, **64**, 408–412.
27 T. Jia, J. Zhang, K. Zhang, H. Tang, S. Dong, C.-H. Tan, X. Wang and F. Huang, *J. Mater. Chem. A*, 2021, **9**, 8975–8983.
28 T. Zhang, Y. Xu, H. Yao, J. Zhang, P. Bi, Z. Chen, J. Wang, Y. Cui, L. Ma, K. Xian, Z. Li, X. Hao, Z. Wei and J. Hou, *Energy Environ. Sci.*, 2023, **16**, 1581–1589.
29 L. Ma, Y. Cui, J. Zhang, K. Xian, Z. Chen, K. Zhou, T. Zhang, W. Wang, H. Yao, S. Zhang, X. Hao, L. Ye and J. Hou, *Adv. Mater.*, 2023, **35**, e2208926.
30 J. Wang, Y. Cui, Y. Xu, K. Xian, P. Bi, Z. Chen, K. Zhou, L. Ma, T. Zhang, Y. Yang, Y. Zu, H. Yao, X. Hao, L. Ye and J. Hou, *Adv. Mater.*, 2022, **34**, e2205009.
31 J. Qu, D. Li, H. Wang, J. Zhou, N. Zheng, H. Lai, T. Liu, Z. Xie and F. He, *Chem. Mater.*, 2019, **31**, 8044–8051.
32 H. Wang, L. Han, J. Zhou, T. Liu, D. Mo, H. Chen, H. Lai, N. Zheng, Z. Xie, W. Zheng and F. He, *CCS Chem.*, 2021, **3**, 2591–2601.
33 C. Sun, J. W. Lee, S. Seo, S. Lee, C. Wang, H. Li, Z. Tan, S. K. Kwon, B. J. Kim and Y. H. Kim, *Adv. Energy Mater.*, 2021, **12**, 2103239.
34 H. Yang, H. Fan, Z. Wang, H. Yan, Y. Dong, C. Cui, H. Ade and Y. Li, *Macromolecules*, 2020, **53**, 9026–9033.
35 H. Wang, H. Chen, W. Xie, H. Lai, T. Zhao, Y. Zhu, L. Chen, C. Ke, N. Zheng and F. He, *Adv. Funct. Mater.*, 2021, **31**, 2100877.
36 Y. Kong, Y. Li, J. Yuan and L. Ding, *InfoMat*, 2022, **4**, e12271.
37 R. Ma, K. Zhou, Y. Sun, T. Liu, Y. Kan, Y. Xiao, T. A. Dela Peña, Y. Li, X. Zou, Z. Xing, Z. Luo, K. S. Wong, X. Lu, L. Ye, H. Yan and K. Gao, *Matter*, 2022, **5**, 725–734.
38 J. W. Lee, C. Sun, D. J. Kim, M. Y. Ha, D. Han, J. S. Park, C. Wang, W. B. Lee, S. K. Kwon, T. S. Kim, Y. H. Kim and B. J. Kim, *ACS Nano*, 2021, **15**, 19970–19980.
39 T. Jia, J. Zhang, H. Tang, J. Jia, K. Zhang, W. Deng, S. Dong and F. Huang, *Chem. Eng. J.*, 2022, **433**, 133575.
40 H. Fu, Q. Fan, W. Gao, J. Oh, Y. Li, F. Lin, F. Qi, C. Yang, T. J. Marks and A. K. Y. Jen, *Sci. China: Chem.*, 2021, **65**, 309–317.
41 H. Yu, Y. Wang, H. K. Kim, X. Wu, Y. Li, Z. Yao, M. Pan, X. Zou, J. Zhang, S. Chen, D. Zhao, F. Huang, X. Lu, Z. Zhu and H. Yan, *Adv. Mater.*, 2022, **34**, e2200361.
42 H. Lai, H. Chen, Y. Zhu, H. Wang, Y. Li and F. He, *Macromolecules*, 2022, **55**, 3353–3360.

43 H. Yu, S. Luo, R. Sun, I. Angunawela, Z. Qi, Z. Peng, W. Zhou, H. Han, R. Wei, M. Pan, A. M. H. Cheung, D. Zhao, J. Zhang, H. Ade, J. Min and H. Yan, *Adv. Funct. Mater.*, 2021, **31**, 2100791.
44 S. Seo, C. Sun, J. W. Lee, S. Lee, D. Lee, C. Wang, T. N. L. Phan, G. U. Kim, S. Cho, Y. H. Kim and B. J. Kim, *Adv. Funct. Mater.*, 2021, **32**, 2108508.
45 H. Sun, B. Liu, Y. Ma, J. W. Lee, J. Yang, J. Wang, Y. Li, B. Li, K. Feng, Y. Shi, B. Zhang, D. Han, H. Meng, L. Niu, B. J. Kim, Q. Zheng and X. Guo, *Adv. Mater.*, 2021, **33**, e2102635.
46 G. Zhang, F. R. Lin, F. Qi, T. Heumuller, A. Distler, H. J. Egelhaaf, N. Li, P. C. Y. Chow, C. J. Brabec, A. K. Jen and H. L. Yip, *Chem. Rev.*, 2022, **122**, 14180–14274.
47 L. Yan, H. Zhang, Q. An, M. Jiang, A. Mahmood, M. H. Jee, H.-R. Bai, H.-F. Zhi, S. Zhang, H. Y. Woo and J.-L. Wang, *Angew. Chem., Int. Ed.*, 2022, **61**, e202209454.
48 Z. Zhou, W. Liu, G. Zhou, M. Zhang, D. Qian, J. Zhang, S. Chen, S. Xu, C. Yang, F. Gao, H. Zhu, F. Liu and X. Zhu, *Adv. Mater.*, 2020, **32**, e1906324.
49 J. Jin, Q. Wang, K. Ma, W. Shen, L. A. Belfiore, X. Bao and J. Tang, *Adv. Funct. Mater.*, 2023, **33**, 2213324.
50 H. Sun, H. Yu, Y. Shi, J. Yu, Z. Peng, X. Zhang, B. Liu, J. Wang, R. Singh, J. Lee, Y. Li, Z. Wei, Q. Liao, Z. Kan, L. Ye, H. Yan, F. Gao and X. Guo, *Adv. Mater.*, 2020, **32**, e2004183.
51 X. Wu, X. Hao, P. Deng and H. Chen, *Dyes Pigm.*, 2021, **196**, 109824.
52 W. Wang, Q. Wu, R. Sun, J. Guo, Y. Wu, M. Shi, W. Yang, H. Li and J. Min, *Joule*, 2020, **4**, 1070–1086.
53 H. R. Bai, Q. An, M. Jiang, H. S. Ryu, J. Yang, X. J. Zhou, H. F. Zhi, C. Yang, X. Li, H. Y. Woo and J. L. Wang, *Adv. Funct. Mater.*, 2022, **32**, 2200807.
54 T. Liu, T. Yang, R. Ma, L. Zhan, Z. Luo, G. Zhang, Y. Li, K. Gao, Y. Xiao, J. Yu, X. Zou, H. Sun, M. Zhang, T. A. Dela Peña, Z. Xing, H. Liu, X. Li, G. Li, J. Huang, C. Duan, K. S. Wong, X. Lu, X. Guo, F. Gao, H. Chen, F. Huang, Y. Li, Y. Li, Y. Cao, B. Tang and H. Yan, *Joule*, 2021, **5**, 914–930.
55 R. Sun, W. Wang, H. Yu, Z. Chen, X. Xia, H. Shen, J. Guo, M. Shi, Y. Zheng, Y. Wu, W. Yang, T. Wang, Q. Wu, Y. Yang, X. Lu, J. Xia, C. J. Brabec, H. Yan, Y. Li and J. Min, *Joule*, 2021, **5**, 1548–1565.
56 F. Zhang, M. Svensson, M. R. Andersson, M. Maggini, S. Bucella, E. Menna and O. Inganäs, *Adv. Mater.*, 2001, **13**, 1871.
57 S. Li, B. Li, X. Yang, H. Wei, Z. Wu, Y. Li, Y. Hu, H. Y. Woo and J. Yuan, *J. Mater. Chem. A*, 2022, **10**, 12997–13004.
58 C. Han, J. Wang, S. Zhang, L. Chen, F. Bi, J. Wang, C. Yang, P. Wang, Y. Li and X. Bao, *Adv. Mater.*, 2023, **35**, e2208986.
59 Y. Li, N. Zheng, L. Yu, S. Wen, C. Gao, M. Sun and R. Yang, *Adv. Mater.*, 2019, **31**, e1807832.
60 C. Han, J. Wang, L. Chen, J. Chen, L. Zhou, P. Wang, W. Shen, N. Zheng, S. Wen, Y. Li and X. Bao, *Adv. Funct. Mater.*, 2021, **31**, 2107026.
61 Y. Li, L. Yu, L. Chen, C. Han, H. Jiang, Z. Liu, N. Zheng, J. Wang, M. Sun, R. Yang and X. Bao, *Innovation*, 2021, **2**, 100090.
62 C. Xiao, X. Wang, T. Zhong, R. Zhou, X. Zheng, Y. Liu, T. Hu, Y. Luo, F. Sun, B. Xiao, Z. Liu, C. Yang and R. Yang, *Adv. Sci.*, 2023, **10**, e2206580.
63 X. Wang, Z. Li, X. Zheng, C. Xiao, T. Hu, Y. Liao and R. Yang, *Adv. Funct. Mater.*, 2023, **33**, 2300323.
64 Z. Li, X. Wang, N. Zheng, A. Saparbaev, J. Zhang, C. Xiao, S. Lei, X. Zheng, M. Zhang, Y. Li, B. Xiao and R. Yang, *Energy Environ. Sci.*, 2022, **15**, 4338–4348.
65 W. Shen, G. Zhao, X. Zhang, F. Bu, J. Yun and J. Tang, *Nanomater.*, 2020, **10**, 944.
66 G. Wang, M. A. Adil, J. Zhang and Z. Wei, *Adv. Mater.*, 2019, **31**, e1805089.
67 J. Han, H. Xu, S. H. K. Paleti, Y. Wen, J. Wang, Y. Wu, F. Bao, C. Yang, X. Li, X. Jian, J. Wang, S. Karuthedath, J. Gorenflot, F. Laquai, D. Baran and X. Bao, *ACS Energy Lett.*, 2022, **7**, 2927–2936.
68 S. Zhang, F. Bi, J. Han, C. Shang, X. Kang and X. Bao, *Nano Energy*, 2022, **102**, 107742.
69 J. Wang, C. Han, J. Han, F. Bi, X. Sun, S. Wen, C. Yang, C. Yang, X. Bao and J. Chu, *Adv. Energy Mater.*, 2022, **12**, 2201614.

